






# Standardized short-term acute heat stress assays resolve historical differences in coral thermotolerance across microhabitat reef sites

Christian R. Voolstra<sup>1,2</sup>  | Carol Buitrago-López<sup>2</sup>  | Gabriela Perna<sup>1,2</sup> |  
 Anny Cárdenas<sup>1,2</sup>  | Benjamin C. C. Hume<sup>2</sup>  | Nils Rådecker<sup>1,2,3</sup>  | Daniel J. Barshis<sup>4</sup> 

<sup>1</sup>Department of Biology, University of Konstanz, Konstanz, Germany

<sup>2</sup>Red Sea Research Center, Division of Biological BESE, King Abdullah University of Science and Technology (KAUST), Thuwal, Saudi Arabia

<sup>3</sup>Laboratory for Biological Geochemistry, School of Architecture, Civil and Environmental Engineering, École Polytechnique Fédérale de Lausanne (EPFL), Lausanne, Switzerland

<sup>4</sup>Department of Biological Sciences, Old Dominion University, Norfolk, VA, USA

## Correspondence

Christian R. Voolstra, Department of Biology, University of Konstanz, 78457 Konstanz, Germany.  
 Email: christian.voolstra@uni-konstanz.de

Daniel J. Barshis, Department of Biological Sciences, Old Dominion University, 110 Mills Godwin Life Sciences Building, Norfolk, VA 23529, USA.  
 Email: dbarshis@odu.edu

## Funding information

King Abdullah University of Science and Technology; Binational Science Foundation, Grant/Award Number: 2016403

## Abstract

Coral bleaching is one of the main drivers of reef degradation. Most corals bleach and suffer mortality at just 1–2°C above their maximum monthly mean temperatures, but some species and genotypes resist or recover better than others. Here, we conducted a series of 18-hr short-term acute heat stress assays side-by-side with a 21-day long-term heat stress experiment to assess the ability of both approaches to resolve coral thermotolerance differences reflective of in situ reef temperature thresholds. Using a suite of physiological parameters (photosynthetic efficiency, coral whitening, chlorophyll *a*, host protein, algal symbiont counts, and algal type association), we assessed bleaching susceptibility of *Stylophora pistillata* colonies from the windward/exposed and leeward/protected sites of a nearshore coral reef in the central Red Sea, which had previously shown differential mortality during a natural bleaching event. Photosynthetic efficiency was most indicative of the expected higher thermal tolerance in corals from the protected reef site, denoted by an increased retention of dark-adapted maximum quantum yields at higher temperatures. These differences were resolved using both experimental setups, as corroborated by a positive linear relationship, not observed for the other parameters. Notably, short-term acute heat stress assays resolved per-colony (genotype) differences that may have been masked by acclimation effects in the long-term experiment. Using our newly developed portable experimental system termed the Coral Bleaching Automated Stress System (CBASS), we thus highlight the potential of mobile, standardized short-term acute heat stress assays to resolve fine-scale differences in coral thermotolerance. Accordingly, such a system may be suitable for large-scale determination and complement existing approaches to identify resilient genotypes/reefs for downstream experimental examination and prioritization of reef sites for conservation/restoration. Development of such a framework is consistent with the recommendations of the

Christian R. Voolstra and Carol Buitrago-López contributed equally to this work.

This is an open access article under the terms of the Creative Commons Attribution License, which permits use, distribution and reproduction in any medium, provided the original work is properly cited.

© 2020 The Authors. *Global Change Biology* published by John Wiley & Sons Ltd

National Academy of Sciences and the Reef Restoration and Adaptation Program committees for new intervention and restoration strategies.

#### KEYWORDS

climate change, coral bleaching, coral reef, heat stress, Red Sea, resilience, thermal stress assay, Coral Bleaching Automated Stress System (CBASS)

## 1 | INTRODUCTION

Coral bleaching caused by ocean warming is among the major drivers of global coral reef decline (De'ath, 2012; Hughes et al., 2017, 2018), and recent years have witnessed the worst global coral bleaching events on record (Hughes et al., 2017). Coral bleaching describes the breakdown of the symbiosis between corals and their photosynthetic symbiotic algae (Symbiodiniaceae; LaJeunesse et al., 2018) under stress (Baker & Cuning, 2015). Because corals lose their primary source of nutrition, bleaching can result in widespread coral mortality. Critical to reef persistence in the future are genotypes, populations, and regions of reef-building corals that can withstand, adapt/acclimate to, or recover from these widespread bleaching events (e.g., Dixon et al., 2015; Guest et al., 2012; Palumbi, Barshis, Traylor-Knowles, & Bay, 2014; van Woesik et al., 2012; van Woesik, Sakai, Ganase, & Loya, 2011).

In recent years, researchers have identified an increasing number of coral populations (e.g., Barshis et al., 2013; Kenkel et al., 2013; Palumbi et al., 2014), reef regions (e.g., Fine, Gildor, & Genin, 2013; Guest et al., 2012; Hume et al., 2013), and individual coral genotypes (e.g., Bay & Palumbi, 2014; Dixon et al., 2015; Lundgren, Vera, Peplow, Manel, & van Oppen, 2013; Osman et al., 2018) that exhibit enhanced bleaching resistance. In some cases, this resistance represents heritable evolutionary variation that could serve as raw material for natural selection or assisted evolution in a changing climate (Dixon et al., 2015; Kenkel, Setta, & Matz, 2015). However, we are missing a standard procedure for determining coral bleaching susceptibility and assessing individuals, populations, and regions for such resilient characteristics. The majority of approaches used are remotely sensed predictions of bleaching occurrence and severity (Liu et al., 2014), observational surveys of naturally occurring bleaching severity and mortality (e.g., Guest et al., 2012), and thermal exposure experiments or in situ field transplantations (e.g., Barshis et al., 2013; Fine et al., 2013; Kenkel et al., 2013; Oliver & Palumbi, 2011; Palumbi et al., 2014). Yet despite these multiple approaches, we have limited understanding on what determines coral bleaching thresholds due to the incompatibility of various methods and a lack of standardization across studies (McLachlan, Price, Solomon, & Grottoli, 2020). Additionally, the commonly used NOAA Coral Reef Watch Degree Heating Weeks hotspot approach (Liu et al., 2014) lacks the spatio-temporal resolution to identify resilience at the scale of the individual coral colony, population, and reef (e.g., Safaie et al., 2018).

Long-term field surveys are one of the most informative measures of bleaching susceptibility, as the frequency and severity of natural bleaching and subsequent recovery are direct measures of the corals' response to an in situ environmental stress. However, natural bleaching

events are difficult to predict (and measure), large-scale bleaching surveys are costly, and monitoring recovery and mortality is a lengthy process requiring months to years of post exposure surveys. Long-term lab exposures (weeks to months) to elevated temperature are designed to approximate the timing and intensity of a natural thermal stress event and have a proven track record in the literature over decades (Jokiel & Coles, 1977); yet these experiments require extensive/expensive aquarium systems capable of sustaining corals for weeks on end. These systems are not practical in many remote locations where coral reefs exist, and the approach takes weeks to months for an assessment of just a single set of individuals from a single population. Recent experiments utilizing short-term (0–3 days), acute thermal exposures in remote field settings show a promising ability to reveal fine-scale differences in thermal tolerance across small spatial scales (Barshis et al., 2013; Bay & Palumbi, 2015; Morikawa & Palumbi, 2019; Palumbi et al., 2014; Ziegler, Seneca, Yum, Palumbi, & Voolstra, 2017).

Here, we assess the performance of such standardized short-term acute heat stress assays in comparison to more commonly employed long-term heat stress experiments to identify differences in bleaching susceptibility across sites and colonies of the coral *Stylophora pistillata*. For this, we directly compared the response of an 18-hr heat stress assay (3 hr heat-ramp, 3 hr heat-hold, 1 hr ramp-down, 11 hr hold) to that of a 21-day long heat stress experiment (14 day acclimation plus 7 days heat-ramp-and-hold) using fragments of the same coral colonies collected from the exposed and protected sites of a nearshore reef in the central Red Sea. Both sites are only 300 m apart, but corals from the warmer and more temperature-variable protected site showed reduced bleaching compared to the colder and less temperature-variable exposed site during a previous natural bleaching event (Pineda et al., 2013). Analysis of a suite of physiological measures demonstrates that both approaches could resolve the putative differences in bleaching sensitivity exhibited after a natural bleaching event. As such, the addition of rapid, field-deployable short-term acute heat stress assays may complement the existing suite of approaches to diagnose thermal tolerance in remote areas at the resolution of single coral colonies.

## 2 | MATERIALS AND METHODS

### 2.1 | Study sites and sample collection

In August 2018, adult colonies of *S. pistillata* were collected from two sites at the nearshore reef Tahala in the central Red Sea, Saudi Arabia (Figure 1). The two sites, designated as Tahala Exposed (windward;

referred to as exposed) site (22.26189°N, 39.04878°E) and Tahala Protected (leeward; referred to as protected) site (22.26302°N, 39.05165°E), are in close proximity to each other (approximately 300 m apart), but exhibit different environmental conditions, in particular with regard to the degree of daily temperature variation (Pineda et al., 2013). Temperature was recorded in 15-min intervals from summer to fall (i.e., from August 2018 to November 2018) for the exposed reef site and from summer to winter (i.e., from August 2018 to February 2019) for the protected reef site (Roik et al., 2016), using in situ deployed HOBO Pendant Temperature Data Loggers (Onset). At each of the two sites, seven coral colonies were sampled using SCUBA at depths of 1–5 m. Colonies were sampled at least 5 m apart from each other to minimize the potential of sampling clonal genotypes (Baums, Miller, & Hellberg, 2006). Sampled specimens were stored in Ziploc plastic bags upon underwater collection and transported to shore in a cooler filled with seawater. All corals were collected under permits from the Saudi Coastguard Authority, issued under the auspices of the King Abdullah University of Science and Technology (KAUST).

## 2.2 | Short-term acute heat stress assays (CBASS)

We used a newly developed portable experimental system termed the Coral Bleaching Automated Stress System (CBASS) to conduct short-term acute heat stress assays (Figure 1, Figure S1). Briefly, the system consists of four replicate 10 L flow-through tanks that allows

running four independent temperature profiles with light settings adjusted to match in situ light fields. The temperature in each tank was controlled by IceProbe Thermoelectric chillers (Nova Tec) and 200W titanium aquarium heaters (Schego) linked to a custom-built controller (Arduino MEGA 2560); the light was controlled manually using an LI-193 Spherical Underwater Quantum Sensor (LI-COR) and manual adjustment of dimmable 165W full spectrum LED aquarium lights (Galaxyhydro) to match reef in situ light fields ( $\sim 600 \mu\text{mol quanta m}^{-2} \text{ s}^{-1}$ ). HOBO Pendant Temperature Data Loggers were used to record the temperature of each tank for the duration of the experiment.

While the CBASS is designed as a portable system with the potential to run assays in the field, for the purpose of comparison to the long-term heat stress experiment it was deployed in the outdoor wet lab facility of the Coastal and Marine Resources Core Lab (CMOR) at KAUST using Red Sea seawater provided by an inflow line. Briefly, collected coral fragments from all seven colonies of both reef sites (exposed, protected) were distributed over the four replicated flow-through tanks, so that fragments from each colony (i.e., genotype) were in each treatment condition ( $2 \times \text{control/baseline} - 30^\circ\text{C}$ ,  $2 \times \text{medium} - 33^\circ\text{C}$ ,  $2 \times \text{high} - 36^\circ\text{C}$ ,  $2 \times \text{extreme} - 39^\circ\text{C}$ ), to make a total of  $2 \times 56$  fragments ( $7 \text{ fragments} \times 2 \text{ sites per tank} = 14$ ;  $14 \text{ fragments per tank} \times 4 \text{ temperatures} = 56 \times 2 \text{ replicated tanks} = 112$ ; all 112 fragments were used for pulse-amplitude modulation (PAM) fluorometry measurements, while for all other analyses a non-replicated

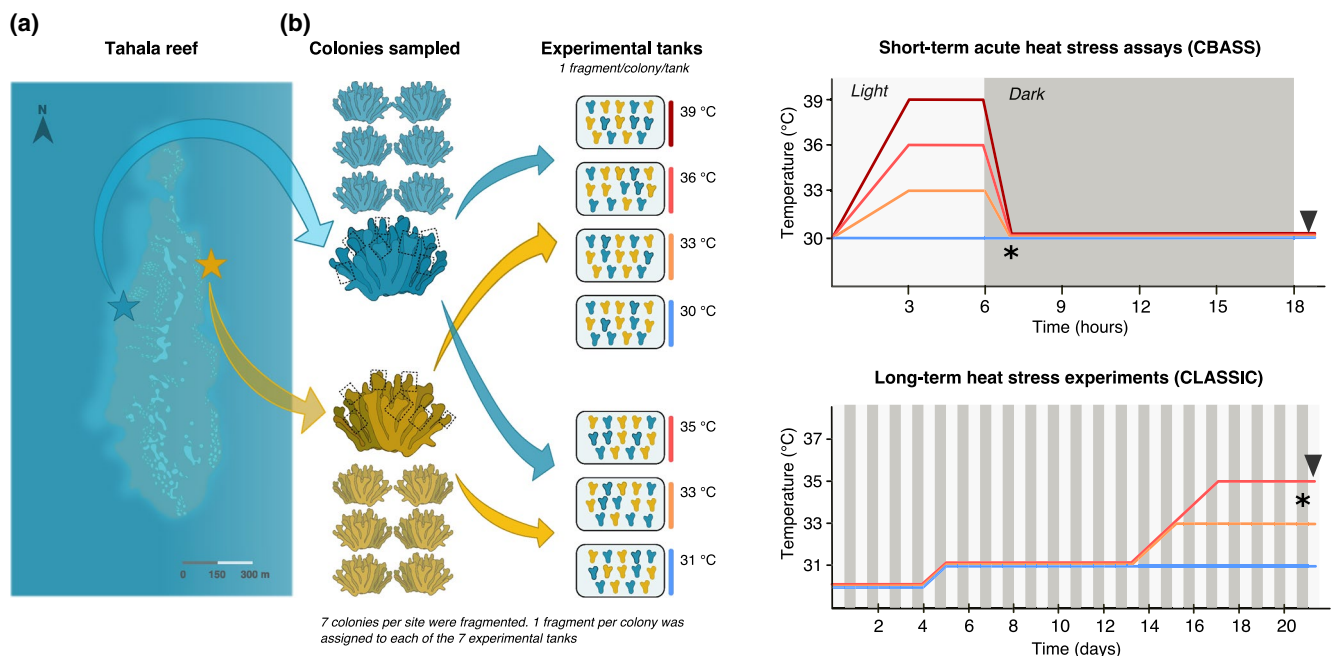


**FIGURE 1** Reef sites and experimental setup. (a) Tahala reef; blue = exposed ocean-facing reef site, orange = protected land-facing reef site; reef sites are approximately 300 m apart. (b) Fragments of seven coral colonies from each of the exposed (blue) and protected (orange) reef sites were collected and subjected to either 18 hr short-term acute heat stress assays (CBASS), run at control ( $30^\circ\text{C}$ ), medium ( $33^\circ\text{C}$ ), high ( $36^\circ\text{C}$ ), and extreme ( $39^\circ\text{C}$ ) temperatures, or 21-day long-term heat stress experiments (14 days acclimation plus 9 days heat stress), run at control ( $31^\circ\text{C}$ ), medium ( $33^\circ\text{C}$ ), and high ( $35^\circ\text{C}$ ) temperatures treatment. Of note, fragments from each coral colony were exposed to each temperature treatment. Asterisks indicate time points of dark-adapted photosynthetic efficiency measurements; arrowheads indicate time points of coral sampling. For reasons of clarity, replicated tanks for each temperature are omitted (see Section 2)

set was used, see below; Figure 1). The start of the experiment was at noon (12:00 hr) and the four treatment conditions were as follows: the control tank was maintained at 30°C for the entire experiment. The three short-term acute heat stress treatment tanks were heated to 33°C, 36°C, and 39°C over a period of 3 hr. The respective temperature was held for 3 hr, and then decreased back to 30°C over the course of 1 hr (19:00 hr). All corals were kept at 30°C overnight until sampling the following morning (08:00 hr), completing the 18-hr short-term acute heat stress assay (August 16, 2018; Figure 1). All tanks were continuously supplied with Red Sea seawater (see above) and photosynthetic active radiation of 600  $\mu\text{mol photons m}^{-2} \text{ s}^{-1}$  on a 12:12 hr day/night cycle.

### 2.3 | Long-term heat stress experiment (CLASSIC)

To compare measurements from the short-term acute heat stress assays to more commonly employed long-term heat stress experiments, we deployed coral fragments from the same 14 collected colonies (see above) across three replicated flow-through aquaria (each 85 L) at the indoor wet lab facility of CMOR at KAUST (50% water renewal per tank per day), so that fragments from each colony (i.e., genotype) were in each treatment condition (2  $\times$  control – 31°C, 2  $\times$  medium – 33°C, 2  $\times$  high – 35°C), to make a total of 2  $\times$  42 fragments (7 fragments  $\times$  2 sites per tank = 14; 14 fragments per tank  $\times$  3 temperatures = 42  $\times$  2 replicated tanks = 84; all 84 fragments were used for PAM fluorometry measurements, while for all other analyses a non-replicated set was used, see below; Figure 1). Tanks were equipped with pumps for constant flow (Aqamai KPS Wavemaker), 600W heaters (SCHEGO Teichheizer), temperature controllers (DD The Aquarium Solution) and HOBO Pendant Temperature Data Loggers. Light intensity was controlled with LED lights (EcoTech Marine Radio XR15FW PRO G2), set to a 12 hr:12 hr day/night cycle according to the “shallow reef” settings of the EcoSmart Live software with maximum quantum irradiance of 182.5  $\mu\text{mol photons m}^{-2} \text{ s}^{-1}$ .

Coral fragments were acclimated at a temperature of 30°C for 4 days, then the temperature was adjusted to 31°C over the course of 1 day to match the maximum monthly mean (MMM) summer temperature for the Central Red Sea as determined from the NOAA Coral Reef Watch 5 km database (Liu et al., 2014). The coral fragments were further acclimated to these conditions for an additional 9 days (Figure 1). For the heat stress experiment, one tank and its replicate remained at 31°C throughout the course of the experiment (control temperature treatment), while for the other two tanks and their respective replicates the temperature was increased by 1°C/day until reaching 33°C (medium temperature treatment) and 35°C (high temperature treatment), respectively. All temperatures were kept for the remainder of the experiment (heat-hold). The experiment was stopped after 21 days (on September 5, 2018) when 50% of the coral fragments at the 35°C treatment showed visible signs of bleaching.

### 2.4 | Photosynthetic efficiency

For measurements of dark-adapted photosynthetic efficiency, experimental tanks for the CBASS and CLASSIC experiments were covered with a tarp at 19:00 hr to ensure complete darkness. After 1 hr (at 20:00 hr), we measured dark-adapted photosynthetic efficiency ( $F_v/F_m$ ) of photosystem II of all coral fragments at all (replicated) temperature treatments using a diving PAM fluorometer (Walz). For CBASS, the measurements were taken after the heat stress and after ramping down to 30°C, whereas for CLASSIC, the measurements were taken on the evening of the day prior to the end of the experiment (Figure 1).

### 2.5 | Photographic assessment of coral chlorophyll contents and whitening

At the end of the CBASS and CLASSIC experiments, all coral fragments were photographed (Nikon 1 J1 with a 10–30 mm VR Lens) with a monochromatic grayscale reference (Kodak Color Separation Guide and Gray Scale Q-13), before being snap-frozen in liquid nitrogen and stored at –80°C until further processing. Red R, Green G, and Blue B pixel intensities were extracted from pictures in MATLAB version 7.10.0 (The MathWorks Inc.) to infer loss of chlorophyll (chl) density (i.e.,  $(\text{chl } a + \text{chl } c_2)/\text{cm}^2$ ) as determined from an increase in pixel intensity of the red channel, following a previously published method (Winters, Holzman, Blekman, Beer, & Loya, 2009). Notably, chl density is a composite measure that comprises the density of symbiotic cells and the chl content within each cell, both of which affect the coral's light capturing abilities, and hence, coral color.

### 2.6 | Coral sample processing and skeletal surface area determination

For physiological and molecular analyses, coral tissue was sprayed off from frozen coral fragments using airflow from a sterile, 1,000  $\mu\text{L}$  pipette tip connected via a rubber hose to a benchtop air pressure valve and ice-cold 0.2  $\mu\text{m}$  filtered seawater (FSW), for a maximum of 3 min. Following this, an aliquot of 100  $\mu\text{L}$  of the tissue slurry was added to 400  $\mu\text{L}$  of Buffer ATL (Qiagen) in a 1.5 ml Eppendorf tube and flash-frozen in liquid nitrogen before being stored at –80°C for subsequent DNA isolation (see below). Spraying continued until all tissue was removed. Tissue slurry was homogenized using a MicroDisTec homogenizer 125 (Thermo Fisher Scientific) and aliquoted for the various physiological measurements as follows: Symbiodiniaceae density 200  $\mu\text{L}$ ; chl *a* 100  $\mu\text{L}$ ; host protein 100  $\mu\text{L}$ ; all aliquots were stored at –20°C. Remaining coral skeletons were retained for surface area determination using the paraffin wax dipping method (Stimson & Kinzie, 1991) with modifications (Holmes, 2008).

## 2.7 | Symbiodiniaceae density, chl *a*, host protein

Symbiodiniaceae cell counts were obtained via flow cytometry (BD LSRFortessa, BD Biosciences). The aliquoted homogenate (see above) was thawed on ice and diluted with 400  $\mu$ l of FSW, vortexed, and passed through a cell strainer (5 ml polystyrene round-bottom tube with cell-strainer cap; Corning Life Sciences). Then, 6  $\mu$ l of 1% sodium dodecyl sulfate (SDS) was added to the strained sample, vortexed, and 300  $\mu$ l were transferred into a 96-well round bottom plate (three technical replicates per sample; Corning Life Sciences) and directly used for flow cytometry analysis. Symbiodiniaceae cells were discriminated from coral host cells and debris by a combination of their forward scatter (size) and red autofluorescence using the FlowJo V 10.5.3 software (TreeStar). The same gating was used for all samples. Symbiodiniaceae triplicate counts were averaged and normalized to the skeletal surface area of the respective coral fragment.

Chl *a* content was determined using absorbance. The aliquoted homogenate (see above) was thawed on ice and centrifuged to separate host and symbiont cells (5,000 *g* for 5 min at 4°C). The supernatant was removed and the symbiont chl extracted via incubation in 100% acetone for 24 hr at 4°C in the dark. Samples were centrifuged (2,000 *g* for 5 min at 4°C) and 200  $\mu$ l were transferred (three technical replicates per sample) to a 96-well flat bottom plate (Greiner, Bio-One). The absorbance was determined at 664, 630, and 750 nm using the SpectraMax Paradigm Multi-Mode Microplate Reader (Molecular Devices). Chl *a* content was then calculated following published methods (Jeffrey & Humphrey, 1975) and corrected for the optical path length (0.555 cm) and normalized to coral surface area denoted as  $\text{cm}^2$ .

The Bradford method was used to analyze host protein content (Bradford, 1976). The homogenate (see above) was thawed on ice, diluted with 400  $\mu$ l of FSW, and centrifuged to separate host and symbiont cells (5,000 *g* for 5 min at 4°C). The supernatant was then transferred to a new 1.5 ml Eppendorf tube and centrifuged further to remove any particulate matter (16,000 *g* for 5 min at 4°C). Three technical replicates per sample (5  $\mu$ l) were mixed with Quick Start Bradford dye reagent (250  $\mu$ l, Bio-Rad) in a 96-well flat bottom plate (Corning Life Sciences) and incubated for 5 min at room temperature. Sample absorbance was measured at 595 nm using the same microplate reader as above and bovine serum albumin was used as the standard. Negative values were set to zero. Measurements were normalized to coral surface area denoted as  $\text{cm}^2$ .

## 2.8 | Statistical analysis

All statistical analyses and data plotting were conducted in R v. 3.5.0 (R Core Team, 2019). Input data and statistical test results are available as supplementary data (Supplementary Data S1, Supplementary Data S2). Further, R scripts and input data are available at <https://github.com/reefgenomics/CBASSvsCLASSIC>. The CBASS and CLASSIC experiments were analyzed separately. For

PAM fluorometry data, statistical analyses were performed using a two-way ANOVA with temperature treatment and reef site as fixed factors and replicated tanks as a random effect. Dark-adapted photosynthetic efficiencies were fitted to a linear mixed model using the *lme4* package (Bates, Mächler, Bolker, & Walker, 2015) and analyzed with ANOVA sum of squares type III as implemented in the *lmerTest* package (Kuznetsova, Brockhoff, & Christensen, 2017). The potential effect of individual colonies was tested by incorporating the colony/genotype as a random effect in a second linear mixed model. To test for a significant colony/genotype effect, we used the function *ranova* of the package *lmerTest* with single term deletions of random-effects. Initial analysis of PAM fluorometry data revealed no significant effect of replicated tanks either for CBASS ( $\chi^2(1) = 0.418$ ,  $p = .517$ ) or CLASSIC ( $\chi^2(1) = 2.84 \times 10^{-14}$ ,  $p = 1$ ) using the function *ranova*. Hence, for all other measurements, two-way ANOVAs sum of squares type III were conducted with temperature treatment and reef site as fixed factors on samples from a single replicate of tanks in order to save sample processing time. ANOVA assumptions of normality and homoscedasticity were assessed by looking at the residuals distribution in quantile–quantile plots and “residuals versus fitted values” & “scale-location” plots, respectively (Kozak & Piepho, 2018). Data transformations (either logarithmic or square-root) were applied to improve the fitting of the model and underlying assumptions where indicated. When there was a significant main effect in the ANOVA including interaction of factors ( $p < .05$ ), post hoc pairwise comparisons of marginal estimated means implemented in the package *emmeans* (Lenth, Singmann, Love, Buerkner, & Herve, 2019) were conducted. This was done in order to determine whether differences between reef sites within each of the respective temperature treatments were statistically significant. P values were adjusted using the Bonferroni correction for multiple comparisons implemented in the R package *stats* (R Core Team, 2019) using the function *p.adjust*. The degree of correlation between the CBASS and CLASSIC experimental setups was assessed independently for each of the physiological parameters tested. For photosynthetic efficiencies, we plotted the relative  $F_v/F_m$  loss comparing medium to control temperatures and high to control temperatures for the CBASS and CLASSIC experiments (averaging over colony replicates at each temperature). For the other physiological parameters, we plotted the respective correlation between the CBASS and CLASSIC experimental setups considering only the difference between high to control temperatures. Linear relationships and correlation coefficients were determined as described above.

## 2.9 | DNA isolation, Symbiodiniaceae ITS2 marker gene sequencing, SymPortal analysis

DNA isolation was performed using the Qiagen DNeasy 96 Blood & Tissue kit (Qiagen) following the manufacturer's instructions with minor adjustments. Briefly, the coral tissue samples aliquoted for DNA isolation (see above) were thawed and equilibrated to room temperature. The slurry was vortexed and 180  $\mu$ l



of each sample was transferred to a microtube with 20  $\mu$ l of proteinase K for incubation at 56°C for 1 hr. DNA extractions were then performed according to the manufacturer's instructions. DNA concentrations were quantified by Qubit (Qubit dsDNA High Sensitivity Assay Kit, Invitrogen). ITS2 (Symbiodiniaceae) amplicon libraries were prepared for sequencing on the Illumina MiSeq platform. To amplify the ITS2 region, the primers SYM\_VAR\_5.8S2 [5'-TCGTCCGGCAGCGTCAGATGTGTATAAGAGACAGGAATTG CAGAACTCCGTGAACC-3'] and SYM\_VAR\_REV [5'-GTCTCGTGG G C T C G G A G A T G T G T A T A A G A G A C A G C G G G T T CWCTTGTYTGACTTCATGC-3'] (Hume et al., 2013, 2015, 2018) were used (Illumina adaptor overhangs underlined). Triplicate PCRs were performed (10–50 ng of DNA from each coral sample) with the Qiagen Multiplex PCR kit, with a final primer concentration of 0.5  $\mu$ M in a final reaction volume of 10  $\mu$ l. Thermal cycler conditions for ITS2 PCR amplification were: initial denaturation at 95°C for 15 min, 30 cycles of 95°C for 30 s, 56°C for 90 s, and 72°C for 30 s, followed by a final extension step of 72°C at 10 min. Then, 5  $\mu$ l of the PCR products were run on a 1% agarose gel to confirm successful amplification. Triplicates for each sample were pooled, and samples were cleaned using ExoProStar 1-step (GE Healthcare). Samples were then indexed using the Nextera XT Index Kit v2 (dual indexes and Illumina sequencing adaptors added). Successful addition of indexes was confirmed by comparing the length of the initial PCR product to the corresponding indexed sample on a 1% agarose gel. Samples were then cleaned and normalized using the SequelPrep Normalization Plate Kit (Invitrogen). The ITS2 libraries were pooled in an Eppendorf tube (4  $\mu$ l per sample) and concentrated using a CentriVap Benchtop Vacuum Concentrator (Labconco). Following this, quality of the library was assessed using the Agilent High Sensitivity DNA Kit on the Agilent 2100 Bioanalyzer (Agilent Technologies). Quantification was done using Qubit (Qubit dsDNA High Sensitivity Assay Kit, Invitrogen). Sequencing was performed at 6 pM with 20% phiX on the Illumina MiSeq platform at 2  $\times$  301 bp paired-end V3 chemistry according to the manufacturer's specifications. Sequence data determined in this study are available under NCBI BioProject PRJNA602678 (<https://www.ncbi.nlm.nih.gov/bioproject/PRJNA602678>). The SymPortal analytical framework was used to analyze the Symbiodiniaceae ITS2 sequence data (Hume et al., 2019; [symportal.org](http://symportal.org)). Briefly, demultiplexed and paired forward and reverse fastq.gz files outputted from the Illumina sequencing were submitted directly to SymPortal. Firstly, sequence quality control was conducted as part of the SymPortal pipeline using mothur 1.39.5 (Schloss et al., 2009), the BLAST+ suite of executables (Camacho et al., 2009), and minimum entropy decomposition (MED; Eren et al., 2014). Then, ITS2 type profiles (representative of putative Symbiodiniaceae taxa or genotypes) were predicted and characterized by specific sets of defining intragenomic ITS2 sequence variants (DIVs). Finally, the ITS2 sequence and ITS2 type profile abundance count tables, as well as the Bray-Curtis-based between-sample and between-ITS2 type profile dissimilarities, as output by the SymPortal analysis, were directly used to plot data. SymPortal ITS2 type profiles and ITS2 relative

sequence abundances over samples are available as supplementary data (Supplementary Data S3). Scripts used for data curation and plotting are available at <https://github.com/reefgenomics/CBASS-vsCLASSIC>.

### 3 | RESULTS

#### 3.1 | Corals from the exposed and protected sites of Tahala reef are exposed to distinct environmental settings

Temperature profiles obtained from in situ deployed loggers for the period from August to November 2018 revealed a similar daily mean water temperature at both sites ( $32.33 \pm 1.21^\circ\text{C}$  and  $32.25 \pm 1.22^\circ\text{C}$ ; mean and standard deviation of exposed and protected sites daily means, respectively) but with a greater diel amplitude at Tahala Protected versus Exposed ( $2.23 \pm 0.59^\circ\text{C}$  vs.  $0.78 \pm 0.42^\circ\text{C}$ , respectively; Figure 2). Consequently, daily maximum temperatures were lower at the exposed site ( $32.61 \pm 1.18^\circ\text{C}$ ) versus the protected site ( $33.65 \pm 1.45^\circ\text{C}$ ), while the opposite was observed for the daily minimum temperature, with higher values for the exposed site ( $31.83 \pm 1.39^\circ\text{C}$ ) versus the protected site ( $31.42 \pm 1.21^\circ\text{C}$ ; Figure 2c,d). As such, despite both reef sites being in very close proximity and seemingly similar as projected from daily temperature means, corals in the protected reef site experience a much more variable and extreme environment, in agreement with findings of Pineda et al. (2013).

#### 3.2 | Corals from the protected site maintain photosynthetic efficiency under heat stress better

We measured dark-adapted photosynthetic efficiency of coral fragments across different temperatures from the exposed and protected sites and inferred that better retention of  $F_v/F_m$  at higher temperatures is representative of higher thermal tolerance (Figure 3). In the CBASS experiment, we observed higher retention of photosynthetic efficiencies in protected versus exposed corals (two-way ANOVA test of site,  $F_{1,100} = 4.259$ ,  $p = .042$ ) and overall lower  $F_v/F_m$  at higher temperatures (two-way ANOVA test of temperature,  $F_{3,4} = 125.354$ ,  $p < .001$ ), although temperature differences between the exposed site ( $\text{emm}_{\text{exposed}} = 0.444$ ,  $\text{SE} = 0.021$ ) and the protected site ( $\text{emm}_{\text{protected}} = 0.513$ ,  $\text{SE} = 0.021$ ) were only significant at  $36^\circ\text{C}$  ( $t_{100} = -2.582$ , Bonferroni-corrected  $p = .045$ ; Figure 3). In the CLASSIC experiment, corals from the protected site also retained a higher photosynthetic efficiency than their exposed site at higher temperatures (two-way ANOVA test of site,  $F_{1,73} = 14.391$ ,  $p < .001$ ), although photosynthetic efficiency decreased at higher temperature (two-way ANOVA test of temperature,  $F_{2,73} = 116.959$ ,  $p < .001$ ), and we found a significant interaction effect between site and temperature (two-way ANOVA test of interaction,  $F_{2,73} = 13.735$ ,  $p < .001$ ). Temperature differences

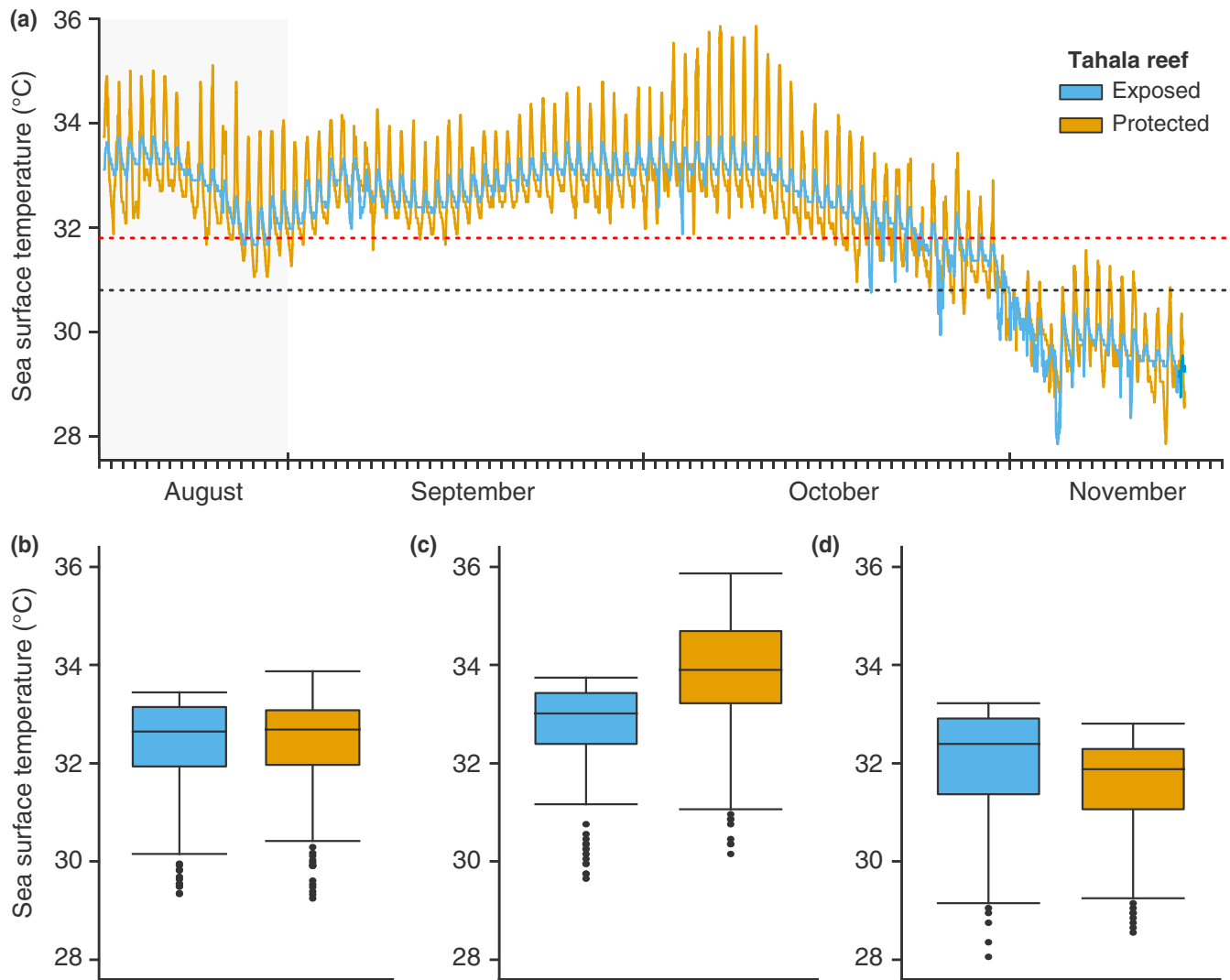


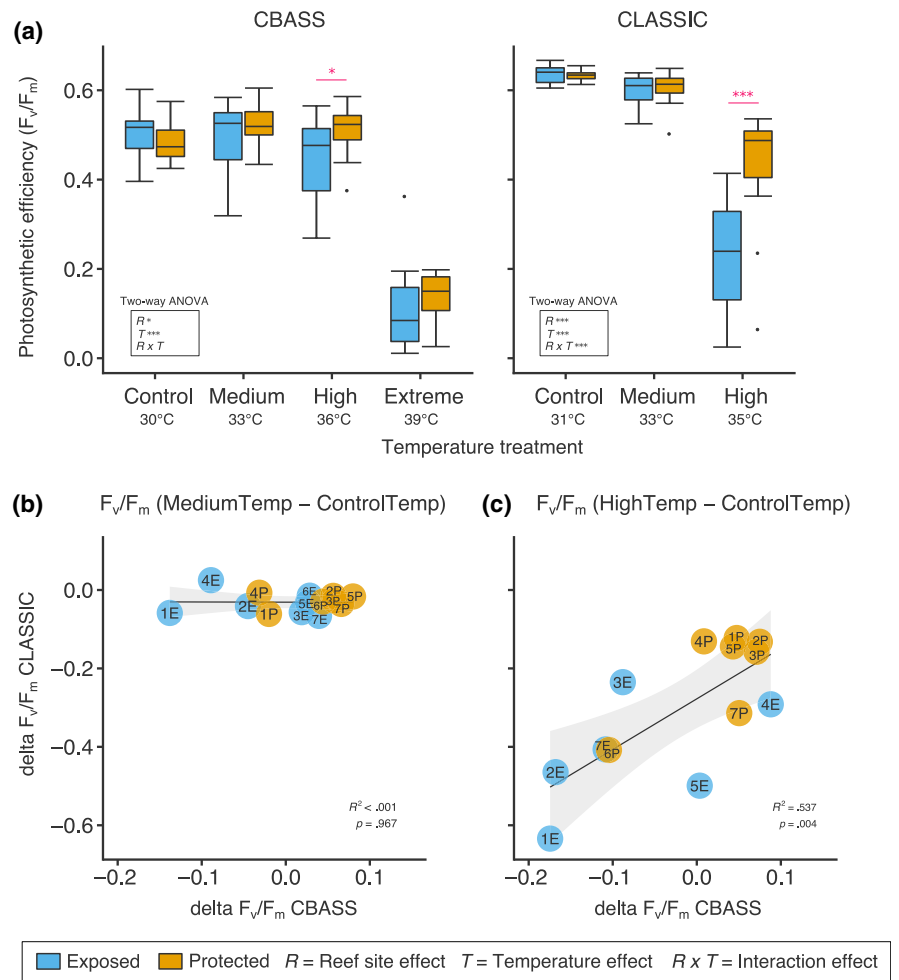
**FIGURE 2** Temperature profiles of the exposed (blue) and protected (orange) sites of Tahala reef in the central Red Sea. (a) Diel temperature profile for the months of August to November 2018 (summer and fall). Dashed black line denotes the maximum monthly mean (30.8°C) according to NOAA Coral Reef Watch, dashed red line denotes the putative bleaching threshold (31.8°C). (b) Daily temperature means. (c) Maximum daily temperatures. (d) Minimum daily temperatures

between the exposed site ( $\text{emm}_{\text{exposed}} = 0.235$ ,  $\text{SE} = 0.0243$ ) and the protected site ( $\text{emm}_{\text{protected}} = 0.431$ ,  $\text{SE} = 0.0203$ ) were only significant at 35°C ( $t_{71.1} = -6.212$ , Bonferroni-corrected  $p < .001$ ; Figure 3a). Notably,  $F_v/F_m$  values were higher in the CLASSIC experiment at control and medium temperatures than in the CBASS experiment (Figure 3a).

To determine the degree of correlation between both experimental setups, we plotted the relative loss of photosynthetic efficiencies of medium and high temperatures in comparison to their control temperatures on a per-colony/genotype basis for CBASS and CLASSIC (Figure 3b,c). While there is no discernible relationship for the medium temperature (Figure 3b), there is a high degree of correlation ( $R^2 = .537$ ,  $p = .004$ ) for the relative loss of  $F_v/F_m$  at the high heat stress temperature for CBASS and CLASSIC (Figure 3c). Notably, coral colonies from the protected site retained photosynthetic efficiency better in both experiments, as indicated by their clustering in the upper right corner of the distribution (Figure 3c). Thus, both

experimental setups resolved the predicted thermal tolerance differences between coral colonies from the exposed and protected sites. Moreover, the plots also reveal the phenotypic variation between coral colonies from a given environment, which seems to be broader for corals from the exposed site as suggested by their wider spread (Figure 3b,c). The observation of colony-level differences was further explored using statistical analysis assessing per-colony/genotype effects for both experimental setups (Supplementary Data S2). While the CBASS experimental setup showed a significant effect of colony/genotype ( $\chi^2(1) = 10.985$ ,  $p < .001$ ), colonies in the CLASSIC experiment did not exhibit significant per-colony differences ( $\chi^2(1) = 1.749$ ,  $p = .185$ ), which may be due to possible acclimation effects in the long-term experiment. Of note, the colony effect is nested in the site effect, and thus, colony correlation between the CBASS and CLASSIC experiments is influenced by the inherent differences between sites, irrespective of a significant per-colony difference (Figure 3c).

**FIGURE 3** Photosynthetic performance under heat stress. (a) Dark-adapted photosynthetic efficiency ( $F_v/F_m$ ) at different heat stress temperatures in the CBASS (left) and CLASSIC (right) experiments. (b, c) Correlation between the CBASS and CLASSIC experimental setups by plotting relative  $F_v/F_m$  loss comparing (b) medium to control temperatures and (c) high to control temperatures. Blue = corals from the exposed site of Tahala reef; orange = corals from the protected site of Tahala reef in the central Red Sea. Colony identities are denoted by their respective ID. Significant differences of two-way ANOVAs testing for reef site, temperature, and a reef site  $\times$  interaction are boxed ( $p \leq .05$ ,  $**p \leq .01$ ,  $***p \leq .001$ ). Pairwise testing denoting significant differences between exposed and protected reef sites for a given temperature are denoted by red asterisks ( $*p \leq .05$ ,  $**p \leq .01$ ,  $***p \leq .001$ ). For the correlation plots: black line = linear regression, grey-shaded area = 95% confidence interval



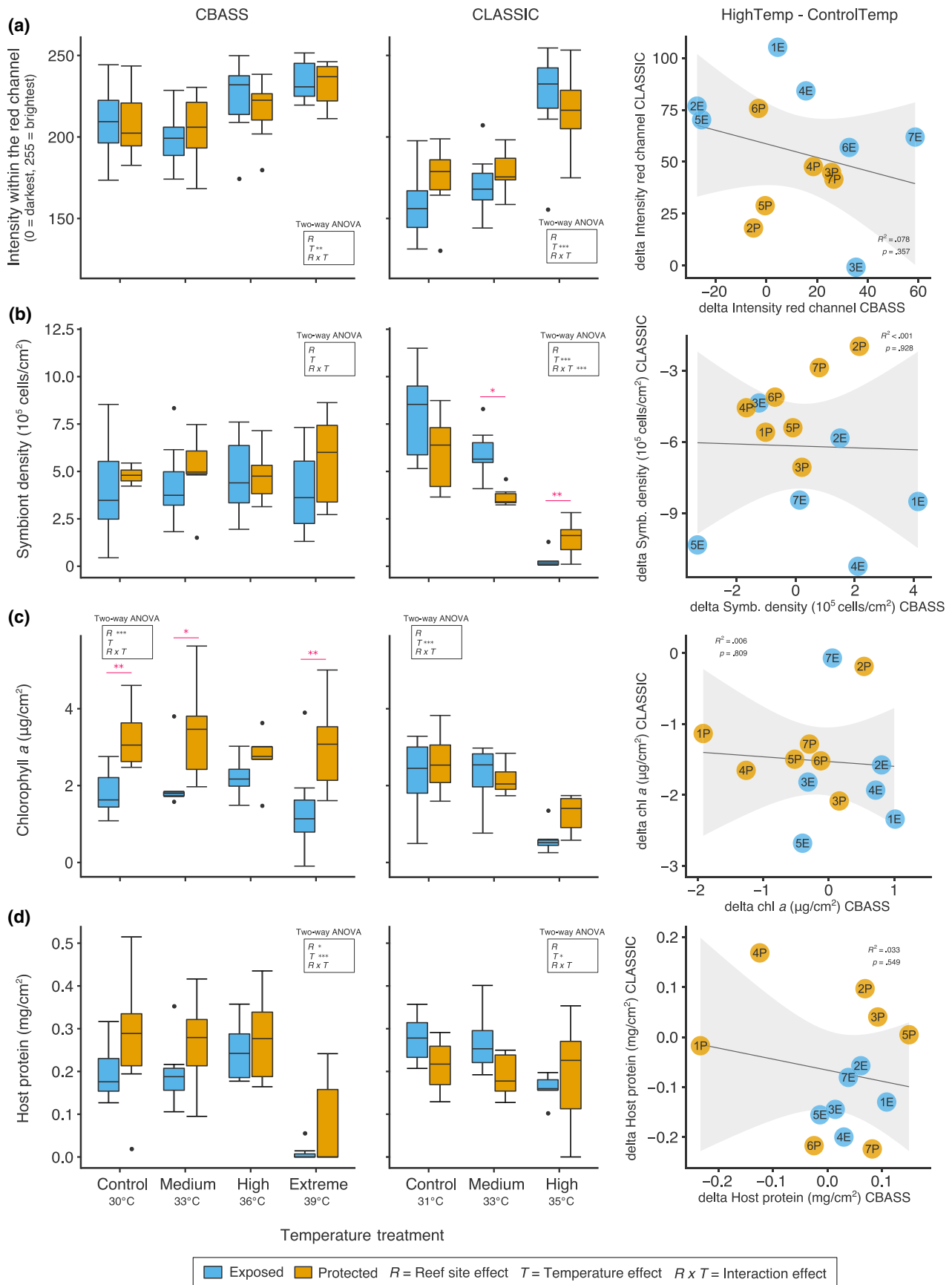
### 3.3 | Loss of chlorophyll density and increased whitening of corals from the exposed and protected sites under heat stress

We determined changes in red pixel intensity of pictures taken from coral fragments to examine the effect of different temperature treatments on relative chl density of corals from the exposed and protected sites (Figure 4a). The method relies on the negative relationship between relative loss of chl density and pixel intensity increase in the red channel in standardized digital photographs (Winters et al., 2009). In the CBASS experiments, corals from the exposed and protected sites displayed a similar increase in red channel pixel intensity, in line with tissue whitening and

loss of chl density (two-way ANOVA test of site,  $F_{1,46} = 0.028$ ,  $p = .867$ ). The loss of chl density was greater at higher temperatures (two-way ANOVA test of temperature,  $F_{3,46} = 5.891$ ,  $p = .002$ ), in line with increased bleaching, yet there was no significant interaction effect between reef sites and temperature treatments (two-way ANOVA test interaction,  $F_{3,46} = 0.201$ ,  $p = .895$ ). Corals in the CLASSIC experiment displayed an overall lower red pixel intensity at control and medium temperatures and a more pronounced increase at the high temperature, although absolute levels at the high and extreme temperature in the CBASS experiment and at the high temperature in the CLASSIC experiment were comparable (Figure 4a). As in the CBASS experiment, corals in the CLASSIC experiment showed a similar loss of

**FIGURE 4** Physiological parameters collected at different heat stress temperatures in the CBASS (left) and CLASSIC (center) experiments and correlation between both experimental setups by plotting relative difference comparing high to control temperatures (right). (a) Red channel pixel intensities of grayscale normalized RGB photographs. An increase in pixel intensity within the red channel is negatively correlated with a relative loss of chl density. (b) Symbiodiniaceae densities. (c) Chl a content ( $\mu\text{g}/\text{cm}^2$ ). (d) Host protein content ( $\text{mg}/\text{cm}^2$ ). Blue = corals from the exposed site of Tahala reef; orange = corals from the protected site of Tahala reef in the central Red Sea. Colony identities are denoted by their respective ID. Significant differences of two-way ANOVAs testing for reef site, temperature, and a reef site  $\times$  interaction are boxed ( $p \leq .05$ ,  $**p \leq .01$ ,  $***p \leq .001$ ). Pairwise testing denoting significant differences between exposed and protected reef sites for a given temperature are denoted by red asterisks ( $*p \leq .05$ ,  $**p \leq .01$ ,  $***p \leq .001$ ). For the correlation plots: black line = linear regression, gray-shaded area = 95% confidence interval





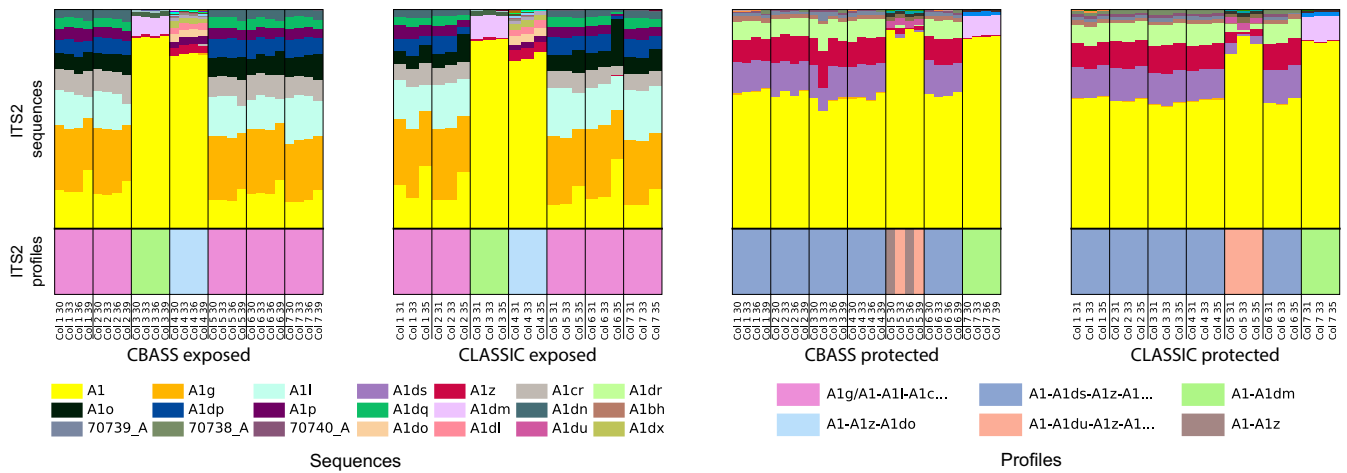


**FIGURE 5** Symbiodiniaceae populations associated with sampled corals. Depicted are the post quality control (post-QC) ITS2 sequences and predicted ITS2 type profiles for each coral specimen. Samples are divided by site (i.e., exposed or protected) and experiment (i.e., CBASS or CLASSIC). For each site/experiment plot, one column represents a single sample at a single temperature, with samples plotted according to the same coral colony/genotype at increasing temperatures. In each column, the relative abundances of ITS2 sequences (post-QC) are plotted above the black line. The relative abundances of predicted ITS2 type profiles are plotted below. For both the ITS2 sequences and the ITS2 type profiles, a full bar represents a relative abundance of 100%

chl density in corals from the exposed and protected reef sites (two-way ANOVA test of site,  $F_{1,35} = 0.499$ ,  $p = .484$ ) with greater lost observed at higher temperatures (two-way ANOVA test of temperature,  $F_{2,35} = 20.374$ ,  $p < .001$ ). In line with the CBASS experiment, there was no significant interaction effect between reef sites and temperature treatments (two-way ANOVA interaction test,  $F_{2,35} = 0.776$ ,  $p = .468$ ).

### 3.4 | Symbiodiniaceae densities retained in CBASS assays and pronounced loss in the CLASSIC experiment

Symbiodiniaceae densities were determined using flow cytometry (Figure 4b). In the CBASS experiment, Symbiodiniaceae densities were  $\sim 10^5$ – $10^6$  cells/cm<sup>2</sup> for corals from both reef sites (two-way ANOVA site test,  $F_{1,48} = 2.816$ ,  $p = .099$ ) and remained relatively constant across temperatures (two-way ANOVA temperature test,  $F_{3,48} = 0.107$ ,  $p = .955$ ; two-way ANOVA interaction test,  $F_{3,48} = 0.319$ ,  $p = .812$ ). Conversely, corals in the CLASSIC experiment exhibited a clear reduction in symbiont densities with increasing temperature (two-way ANOVA temperature test,  $F_{2,35} = 92.757$ ,  $p < .001$ ) and highly significant differences in symbiont densities at 33°C and 35°C between sites (two-way ANOVA interaction test,  $F_{2,35} = 10.657$ ,  $p < .001$ ). Interestingly, corals from the exposed site had significantly higher symbiont densities at 33°C ( $\text{emm}_{\text{exposed}} = 593,826$ ,  $SE = 65,240$  vs.  $\text{emm}_{\text{protected}} = 364,037$ ,  $SE = 51,081$ ;  $t_{35} = 2.794$ ,  $p = .025$ ), whereas corals from the protected site had significantly higher symbiont densities at 35°C ( $\text{emm}_{\text{exposed}} = 24,594$ ,  $SE = 14,341$  vs.  $\text{emm}_{\text{protected}} = 128,106$ ,  $SE = 30,302$ ;  $t_{35} = -3.227$ ,  $p = .008$ ; Figure 4b).

### 3.5 | Higher chl *a* content in corals from the protected site in CBASS assays and overall loss of chl *a* in the CLASSIC experiment

In the CBASS assays, corals from the protected site exhibited significantly higher amounts of chl *a*/cm<sup>2</sup> in comparison to their exposed site counterparts (two-way ANOVA site test,  $F_{1,47} = 22.497$ ,  $p < .001$ ), as confirmed by significant differences between sites for all temperatures except for the corals at 36°C (Figure 4c). Amounts of chl *a* were consistent across temperatures (two-way ANOVA temperature test,  $F_{3,47} = 0.401$ ,  $p = .753$ ) and showed no temperature-site interaction (two-way ANOVA interaction test,  $F_{3,47} = 0.742$ ,  $p = .532$ ), resembling the pattern for symbiont densities (Figure 4b). In the CLASSIC experiment, levels of chl *a* were similar between protected and exposed sites (two-way ANOVA site test,  $F_{1,35} = 3.701$ ,  $p = .0625$ ) but, in contrast to the CBASS experiment, showed a clear reduction with increasing temperature (two-way ANOVA temperature test,  $F_{2,35} = 20.855$ ,  $p < .001$ ). Notably, at 35°C, corals from the protected site seemed to retain higher amounts of chl *a* than the exposed site, but this difference was not statistically significant ( $\text{emm}_{\text{protected}} = 1.225 \mu\text{g}/\text{cm}^2$ ,  $SE = 0.162$  vs.  $\text{emm}_{\text{exposed}} = 0.569 \mu\text{g}/\text{cm}^2$ ,  $SE = 0.162$ ;  $t_{35} = -2.402$ ,  $p = .065$ ; Figure 4c).

### 3.6 | Differential patterns of retention and loss of host protein content between CBASS and CLASSIC experiments

In the CBASS experiment, we found a higher protein content in corals from the protected site compared to corals from the exposed site (two-way ANOVA site test,  $F_{1,48} = 4.057$ ,  $p = .049$ ; Figure 4d). Although retention of host protein content seemed higher in corals from the

protected site (in particular at 39°C), in line with a higher thermotolerance, no significant interaction effect was found (two-way ANOVA interaction test,  $F_{3,48} = 0.412$ ,  $p = .745$ ), possibly due to variability across coral colonies (Figure 4d). Corals in the CLASSIC experiment, by comparison, had overall similar protein content regardless of site (two-way ANOVA site test,  $F_{1,35} = 2.503$ ,  $p = .122$ ). Overall, host protein content was comparable to the CBASS assays and was retained in corals from the protected site across temperatures.

### 3.7 | Distinct Symbiodiniaceae community composition of corals from exposed and protected sites

Analysis of the Symbiodiniaceae community composition based on next-generation sequencing of the ITS2 region using SymPortal (Hume et al., 2019) revealed that distinct microalgal genotypes were associated with the majority of *S. pistillata* colonies from the exposed and protected sites (Figure 5). Corals from the exposed site were primarily associated with symbionts of the ITS2 type profile A1g/A1-A1l-A1cr-A1o-A1dp-A1p-A1dq-A1dn (five colonies), and to a lesser extent A1-A1dm (one colony) and A1-A1z-A1do (one colony). Corals from the protected site were primarily associated with algal symbionts of the ITS2 type profile A1-A1ds-A1z-A1dr-A1bh (five colonies), and to a lesser extent A1-A1dm (one colony) and A1-A1du-A1z-A1ds-A1dr (one colony). Notably, for every coral colony, symbiont association was consistent across temperatures and between CBASS assays and the CLASSIC experiment, except for one colony from the protected site and only in the CBASS assay (Figure 5). We consider this an analytical artifact, as supported by the unanimous profiles for the same colony in the CLASSIC experiment (Figure 5). Notably, SymPortal assigns ITS2 type profiles, which do not necessarily translate into different symbiont species. Nevertheless, as alluded above, symbiont association was not uniform for corals from the exposed and protected reef sites. One colony from the exposed site (colony 3) and one colony from the protected site (colony 7) even harbored the same symbiont type profile (A1-A1dm), suggesting that inference of symbiont genotypes from site-associated thermal tolerance phenotypes is not absolute and other factors are at play that deserve consideration.

## 4 | DISCUSSION

### 4.1 | A standardized portable experimental system and framework for in situ assessment of coral thermal tolerance

Here, we sought to develop a standardized, cost-effective, and experimentally validated suite of rapid, field-deployable short-term acute heat stress assays, which we termed CBASS (Figure 1; Figure S1). Our intent was to examine whether CBASS short-term acute heat stress assays are informative with regard to in situ coral thermal tolerance differences and to what extent CBASS assays are comparable to more

commonly conducted long-term heat stress experiments. We define thermal tolerance as the ability of the coral holobiont to survive heat stress, and we refer to tolerant coral holobionts as those that are able to maintain physiological performance and an intact symbiosis during heat stress better than others. We focused on thermal tolerance as it is straightforward to measure in portable short-term heat stress experimental setups that can be deployed across large spatial scales. For the purpose of a proof-of-principle, we chose the nearshore reef Tahala in the central Red Sea that was previously shown to exhibit differences in thermal tolerance of corals from its exposed/windward and protected/leeward sites (Pineda et al., 2013). We confirmed a higher thermal tolerance of corals from the protected site in both experimental setups, that is, short-term acute heat stress assays and long-term heat stress experiments, using a suite of physiological parameters. Importantly, the physiological parameters differed in their ability to resolve thermal tolerance differences across fine-scale geographical settings and this was also dependent on the experimental setup, as discussed below.

### 4.2 | Performance of different physiological measures of experimental heat stress as a proxy for in situ thermal tolerance

Results from both the CBASS and CLASSIC experimental setups using dark-adapted maximum quantum yield ( $F_v/F_m$ ) as a proxy for thermotolerance suggest that corals from the protected site are less photosynthetically stressed at higher temperatures than corals from the exposed site (Figure 3). Both experimental setups showed higher retention of  $F_v/F_m$  in corals from the protected versus exposed site at increasing temperatures (Figure 3), suggesting that corals that perform better in short-term acute heat stress assays also fare better in long-term heat stress experiments. Of note,  $F_v/F_m$  values in the CLASSIC experiment were higher overall at control and medium temperatures in comparison to the CBASS experiments. This may be attributable to acclimation to the aquaria conditions (e.g., lower light). The more pronounced loss of photosynthetic efficiency at 35°C in the CLASSIC experiment in comparison to the 36°C in the CBASS assays, may also be interpreted as the cost of accumulated stress under a long-term heat stress.  $F_v/F_m$  is commonly used as a non-invasive proxy for coral stress prior to colony paling (Warner, Fitt, & Schmidt, 1996), however the exact mechanisms involved in the bleaching response and the specific role of the breakdown of photosystem II integrity remain an area of active research (Warner, Lesser, & Ralph, 2010). Here, we show consistent agreement between a greater decline in  $F_v/F_m$  in exposed corals in our experimental heat stresses and a greater incidence of bleaching in exposed corals in the in situ 2010 bleaching event examined by Pineda et al. (2013). While this is far from a causal relationship, Morikawa & Palumbi (2019) also observed correlation between reduced bleaching in short-term acute heat stress assays and reduced bleaching during an in situ warming event. Taken together, these results suggest that greater retention of  $F_v/F_m$  during acute heat stress exposures may be a useful proxy for higher thermal tolerance/increased bleaching resistance during natural stress events, regardless of the specific causal mechanism.

Using red pixel intensity-inferred chl density, we found a decrease (i.e., whitening) with increasing temperature in both the CBASS and CLASSIC experiments. Consequently, this measure might work to document relative bleaching of coral fragments, but we could not resolve statistically significant site-specific differences. A decrease in Symbiodiniaceae density (Figure 4b) and chl *a* content (Figure 4c) are common measures to denote coral bleaching, but a decrease with increasing temperature could only be resolved in the long-term experiment. Conversely, chl *a* (Figure 4c) and host protein (Figure 4d) content resolved site-specific differences in the CBASS experiment. The coral bleaching response involves a complex cascade of processes thought to begin with intracellular reactive oxygen species generation by both host mitochondria and symbiont chloroplasts (e.g., Lesser, 2006; Lesser, Stochaj, Tapley, & Shick, 1990). This is followed by intercellular breakdown of the integrity of the symbiosis and dissociation of the two partners (e.g., Bieri, Onishi, Xiang, Grossman, & Pringle, 2016; Gates, Baghdasarian, & Muscatine, 1992). Thus, we view the loss of chl *a* and symbiont cells as an integration of multiple stress responses and stress-induced damage across the entire organism versus  $F_v/F_m$  as a specific measure of the light harvesting capability of photosystem II. Consequently, Symbiodiniaceae density and chl *a* content may not be appropriate physiological parameters to resolve fine-scale differences in thermal tolerance using short-term heat stress assays, although further testing is underway.

With regard to host protein content, we found significant differences between exposed and protected sites in the CBASS experiment, with higher protein content in corals from the protected site, indiscriminate of temperature. In the extreme temperature treatment, corals exhibited substantial protein loss, which likely reflects greater loss of host tissue due to necrosis and sloughing. In the CLASSIC experiment, there was only an effect of temperature (but not site), likely resulting from a few individuals with lower protein content at the high temperature. Despite its broad utilization, total protein is a rather coarse measure to assess tissue biomass, as protein content is only one component of total tissue biomass (Edmunds, Gates, & Gleason, 2003). Thus, as with Symbiodiniaceae density and chl *a*, host protein may not be as responsive or precise a measure as  $F_v/F_m$  to resolve fine-scale differences in thermal tolerance, though the consistent difference between sites in the CBASS samples raise the possibility of steady-state differences in tissue composition between sites that may influence thermal responses.

Taken together, despite the good agreement in results from PAM fluorometry measurements, it becomes evident that there is an overall lack of correlation between CBASS and CLASSIC experiments for the remaining parameters evaluated, i.e., red channel pixel intensity, symbiont density, chl *a* levels, and host protein content (Figure 4a–d correlation plots). Importantly, this does not necessarily reflect on the efficacy of these parameters to resolve thermotolerance differences—e.g., site-specific differences were resolved using chl *a* and host protein in CBASS, and temperature-specific differences were resolved using symbiont density and chl *a* in CLASSIC—but that these parameters respond differently in short- and long-term experimental setups. Conversely, we argue that we find a good correspondence between

both experimental setups using PAM fluorometry because maintaining photosynthetic efficiency levels under heat stress indicates the ability of the coral holobiont to maintain a suitable environment for its microalgal symbionts which manifests in both short- and long-term experiments. Importantly, the observed alignment between a reduction in photosynthetic efficiency and heat stress susceptibility of corals does not imply a (sole) causal role of photosynthetic impairment in the bleaching response of corals (Gardner et al., 2017; Nielsen, Petrou, & Gates, 2018; Ralph, Gademann, & Larkum, 2001). Rather, as outlined above, we argue that the ability to maintain photosynthetic efficiency under heat stress is an overall indicator of heat stress resilience. Hence, although (short-term) declines in photosynthetic efficiency may be symptomatic rather than causative, they are indicative of a reduced thermal tolerance temperature threshold. Accordingly, PAM fluorometry measurements provide an inexpensive, indicative, and non-intrusive method/tool to identify thermal tolerance differences in corals, and are particularly well-suited for use in short-term acute heat stress assays. It will be interesting to determine which other physiological parameters are suitable to consistently reveal differences in thermal tolerance using short- and long-term heat stress experimental setups.

#### 4.3 | Differences in thermal tolerance reflected by microalgal association

Analysis of the ITS2 region using the SymPortal analytical framework resolved distinct differences in the algal symbiont composition between the exposed and protected sites. Notably, algal symbiont composition was not uniform within sites. Rather it seems that putatively different symbiont species associate with corals in both locations, although the majority of corals from both sites harbored the same symbiont profile(s) that differed from the opposing site. Given the uncertainty associated with assigning a contribution of holobiont thermal tolerance to specific symbionts genotypes/species (with some notable exceptions, e.g., Hume et al., 2016; LaJeunesse et al., 2014), we conclude that it is not a suitable parameter to determine ad hoc differences in thermal tolerance. Nevertheless, symbiont identity may be one of the putative components that underlie the observed differences in bleaching susceptibility between the two sites.

#### 4.4 | Environmental factors that shape thermal tolerance and the importance of microhabitats

The common notion is that corals are adapted to their latitudinal climate and bleach and suffer mortality at just 1–2°C above their mean sea surface temperature of the hottest month (MMM) temperatures (Glynn & D'Croz, 1990; Jokiel, 2004), but we actually know little about empirical temperature thresholds in corals and what is shaping them. Indeed, recent thermal history (Middlebrook, Hoegh-Guldberg, & Leggat, 2008), microhabitat heterogeneity (Oliver & Palumbi, 2011; Palumbi et al., 2014; Safaie et al., 2018), and taxonomic identity of

the individual coral holobiont members (Hume et al., 2015; Rosado et al., 2019; Ziegler et al., 2017) have been shown to contribute to, and even surpass, differences in thermal thresholds attributed to latitudinal adaptation (Jokiel & Coles, 1990), which is further supported by our study. Despite both of our study sites being only hundreds of meters apart and exhibiting a similar daily mean water temperature, the protected reef site is subject to a more extreme and variable environment, as indicated by the overall warmer and cooler water temperatures and larger diel fluctuations (Figure 2). In line with these environmental differences, corals from the more variable protected site of Tahala reef showed increased survival after a previous bleaching event, presumably resulting from higher thermal tolerance (Pineda et al., 2013). Indeed, such microhabitat differences were shown to contribute to differential patterns of thermal tolerance in previous studies. For instance, corals from nearby reef sites on Ofu Island (American Samoa) that showed similar temperature fluctuations and differences to those documented here exhibited different thermal tolerances, i.e., corals from the more variable/extreme environment(s) were less bleaching susceptible (Oliver & Palumbi, 2011; Palumbi et al., 2014; Safaie et al., 2018). As such, the importance of microhabitats in shaping patterns of thermal tolerance should be further explored. Importantly, only the recording of high resolution in situ temperature data revealed the highly variable and extreme diel differences, which are not accessible from remote sensing data focusing on mean temperature over larger time spans. Along this line, the MMM (summer) temperature for Tahala reef is 30.8°C as determined by the NOAA Coral Reef Watch, 5 km global product (Liu et al., 2014), providing 31.8°C as a putative bleaching threshold. Yet, corals from both sites spend a significant amount of their lifetime above such remote sensing predicted bleaching thresholds (Figure 2), making a strong case for at site in situ experimental approaches to complement remote sensing methods in determining regional bleaching thresholds. There are two further things to note: (i) Six years after the study by Pineda et al. (2013), we could recapitulate expected differences in coral thermal tolerance between sites. As such, small-scale environmental heterogeneity seems to predictably shape thermal tolerance, irrespective of the occurrence of (selective) bleaching events (*sensu* Guest et al., 2012), and (ii) despite putative differential selection of stress-tolerant genets, we still find substantial biological variance between coral colonies at both sites. This suggests that a multitude of environmental factors contribute to the success and persistence of coral holobionts, and we currently have a limited understanding of these factors and how they contribute to stress tolerance.

#### 4.5 | Standardized in situ heat stress assays as a means to diagnose resilient corals and genotypes across their global distribution

Given the ongoing degradation of coral reef ecosystems worldwide (Hughes et al., 2018), the identification of stress-tolerant reefs and corals becomes an important priority—be it as targets for direct conservation efforts, or as source material for restoration and further

efforts (e.g., coral probiotics, selective crossing, assisted evolution; National Academies of Sciences Engineering & Medicine, 2019). This is to say that coral populations (e.g., Barshis et al., 2013; Kenkel et al., 2013; Palumbi et al., 2014), reef regions (e.g., Fine et al., 2013; Guest et al., 2012; Osman et al., 2018), and individual coral genotypes (e.g., Bay & Palumbi, 2014; Dixon et al., 2015; Lundgren et al., 2013) with enhanced bleaching resistance exist, but the challenge of identifying them remains. A standardized, portable experimental system such as CBASS allows identification of thermally tolerant coral populations on site and in their native environment, which will then allow for downstream targeted investigations into the genetic/genomic makeup of thermal tolerance. Understanding how and which corals survive thermal stress events and gaining knowledge about the underlying holobiont features will rationally inform action on conservation and restoration efforts at local, regional, and global scales. Ultimately, the goal is to expand upon the proposed efforts with more advanced stress testing to determine which thermal tolerance signatures also predict resilience.

#### ACKNOWLEDGEMENTS

Part of this study was conducted as the master's thesis of G.P. This project was supported by research funding from King Abdullah University of Science and Technology to C.R.V. and a Binational Science Foundation award (2016403) to D.J.B. We would like to thank Katherine Rowe for assistance with field and lab work. We would also like to thank the Bioscience Core Lab (BCL) for sequencing and CMOR for assistance with aquaria experiments and boating operations, in particular Zenon Batang and Nabeel Alikuhni.

#### CONFLICT OF INTEREST

The authors declare no conflict of interest.

#### AUTHOR CONTRIBUTIONS

C.R.V., C.B.-L., and D.J.B. designed and conceived the experiments. C.R.V. and D.J.B. provided reagents/tools. C.R.V., C.B.-L., G.P., A.C., N.R., and D.J.B. generated data. C.R.V., C.B.-L., G.P., B.C.C.H., N.R., and D.J.B. analyzed and interpreted the data. C.R.V., C.B.-L., G.P., and D.J.B. wrote the manuscript with contributions from all authors.

#### DATA AVAILABILITY STATEMENT

Data and scripts from this study are available as Supplementary Data and at <https://github.com/reefgenomics/CBASSvsCLASSIC>. Raw ITS2 sequencing data determined in this study is accessible at NCBI under BioProject ID PRJNA602678 (<https://www.ncbi.nlm.nih.gov/bioproject/PRJNA602678>).

#### ORCID

Christian R. Voolstra  <https://orcid.org/0000-0003-4555-3795>

Carol Buitrago-López  <https://orcid.org/0000-0001-5985-5837>

Anny Cárdenas  <https://orcid.org/0000-0002-4080-9010>

Benjamin C. C. Hume  <https://orcid.org/0000-0001-7753-3903>

Nils Rådecker  <https://orcid.org/0000-0002-2387-8567>

Daniel J. Barshis  <https://orcid.org/0000-0003-1510-8375>



## REFERENCES

- Baker, A. C., & Cuning, R. (2015). Coral "Bleaching" as a generalized stress response to environmental disturbance. In J. W. Porter, S. B. Galloway, A. W. Bruckner, C. M. Woodley, & C. Downs (Eds.), *Diseases of coral* (Issue 800, pp. 396–409). John Wiley & Sons, Inc. <https://doi.org/10.1002/9781118828502.ch30>
- Barshis, D. J., Ladner, J. T., Oliver, T. A., Seneca, F. O., Traylor-Knowles, N., & Palumbi, S. R. (2013). Genomic basis for coral resilience to climate change. *Proceedings of the National Academy of Sciences of the United States of America*, 110(4), 1387–1392. <https://doi.org/10.1073/pnas.1210224110>
- Bates, D., Mächler, M., Bolker, B., & Walker, S. (2015). Fitting linear mixed-effects models using lme4. *Journal of Statistical Software*, 1(1), 2015. Retrieved from <https://www.jstatsoft.org/v067/i01>
- Baums, I. B., Miller, M. W., & Hellberg, M. E. (2006). Geographic variation in clonal structure in a reef-building Caribbean coral, *Acropora palmata*. *Ecological Monographs*, 76(4), 503–519. [https://doi.org/10.1890/0012-9615\(2006\)076\[0503:GVICSJ\]2.0.CO;2](https://doi.org/10.1890/0012-9615(2006)076[0503:GVICSJ]2.0.CO;2)
- Bay, R. A., & Palumbi, S. R. (2014). Multilocus adaptation associated with heat resistance in reef-building corals. *Current Biology*, 24(24), 2952–2956. <https://doi.org/10.1016/j.cub.2014.10.044>
- Bay, R. A., & Palumbi, S. R. (2015). Rapid acclimation ability mediated by transcriptome changes in reef-building corals. *Genome Biology and Evolution*, 7(6), 1602–1612. <https://doi.org/10.1093/gbe/evv085>
- Bieri, T., Onishi, M., Xiang, T., Grossman, A. R., & Pringle, J. R. (2016). Relative contributions of various cellular mechanisms to loss of algae during cnidarian bleaching. *PLoS ONE*, 11(4). <https://doi.org/10.1371/journal.pone.0152693>
- Bradford, M. M. (1976). A rapid and sensitive method for the quantitation of microgram quantities of protein utilizing the principle of protein-dye binding. *Analytical Biochemistry*, 72(1), 248–254. [https://doi.org/10.1016/0003-2697\(76\)90527-3](https://doi.org/10.1016/0003-2697(76)90527-3)
- Camacho, C., Coulouris, G., Avagyan, V., Ma, N., Papadopoulos, J., Bealer, K., & Madden, T. L. (2009). BLAST+: Architecture and applications. *BMC Bioinformatics*, 10, 421. <https://doi.org/10.1186/1471-2105-10-421>
- De'ath, G., Fabricius, K. E., Sweatman, H., & Puotinen, M. (2012). The 27-year decline of coral cover on the Great Barrier Reef and its causes. *Proceedings of the National Academy of Sciences of the United States of America*, 109(44), 17995–17999. <https://doi.org/10.1073/pnas.1208909109>
- Dixon, G. B., Davies, S. W., Aglyamova, G. A. V., Meyer, E., Bay, L. K., & Matz, M. V. (2015). Genomic determinants of coral heat tolerance across latitudes. *Science*, 348(6242), 1460–1462. <https://doi.org/10.1126/science.1261224>
- Edmunds, P. J., Gates, R. D., & Gleason, D. F. (2003). The tissue composition of *Montastraea franksi* during a natural bleaching event in the Florida Keys. *Coral Reefs*, 22(1), 54–62. <https://doi.org/10.1007/s00338-003-0278-5>
- Eren, A. M., Morrison, H. G., Lescault, P. J., Reveillaud, J., Vineis, J. H., & Sogin, M. L. (2014). Minimum entropy decomposition: Unsupervised oligotyping for sensitive partitioning of high-throughput marker gene sequences. *The ISME Journal*, 9(4), 968–979. <https://doi.org/10.1038/ismej.2014.195>
- Fine, M., Gildor, H., & Genin, A. (2013). A coral reef refuge in the Red Sea. *Global Change Biology*, 19(12), 3640–3647. <https://doi.org/10.1111/gcb.12356>
- Gardner, S., Raina, J.-B., Nitschke, M., Nielsen, D., Stat, M., Motti, C., ... Petrou, K. (2017). A multi-trait systems approach reveals a response cascade to bleaching in corals. *BMC Biology*, 15, 117. <https://doi.org/10.1186/s12915-017-0459-2>
- Gates, R. D., Baghdasarian, G., & Muscatine, L. (1992). Temperature stress causes host cell detachment in symbiotic cnidarians: Implications for coral bleaching. *Biological Bulletin*, 182(3), 324–332. <https://doi.org/10.2307/1542252>
- Glynn, P. W., & D'Croz, L. (1990). Experimental evidence for high temperature stress as the cause of El Niño-coincident coral mortality. *Coral Reefs*, 8(4), 181–191. <https://doi.org/10.1007/BF00265009>
- Guest, J. R., Baird, A. H., Maynard, J. A., Muttaqin, E., Edwards, A. J., Campbell, S. J., ... Chou, L. M. (2012). Contrasting patterns of coral bleaching susceptibility in 2010 suggest an adaptive response to thermal stress. *PLoS ONE*, 7(3), e33353. <https://doi.org/10.1371/journal.pone.0033353>
- Holmes, G. (2008). Estimating three-dimensional surface areas on coral reefs. *Journal of Experimental Marine Biology and Ecology*, 365(1), 67–73. <https://doi.org/10.1016/j.jembe.2008.07.045>
- Hughes, T. P., Anderson, K. D., Connolly, S. R., Heron, S. F., Kerry, J. T., Lough, J. M., ... Wilson, S. K. (2018). Spatial and temporal patterns of mass bleaching of corals in the Anthropocene. *Science*, 359(6371), 80–83. <https://doi.org/10.1126/science.aan8048>
- Hughes, T. P., Kerry, J., Álvarez-Noriega, M., Álvarez-Romero, J., Anderson, K., Baird, A., ... Wilson, S. (2017). Global warming and recurrent mass bleaching of corals. *Nature*, 543, 373–377. <https://doi.org/10.1038/nature21707>
- Hume, B., D'Angelo, C., Burt, J., Baker, A. C., Riegl, B., & Wiedenmann, J. (2013). Corals from the Persian/Arabian Gulf as models for thermotolerant reef-builders: prevalence of clade C3 symbiodinium, host fluorescence and ex situ temperature tolerance. *Marine Pollution Bulletin*, 72(2), 313–322. <https://doi.org/10.1016/j.marpolbul.2012.11.032>
- Hume, B., D'Angelo, C., Smith, E. G., Stevens, J. R., Burt, J., & Wiedenmann, J. (2015). *Symbiodinium thermophilum* sp. nov., a thermotolerant symbiotic alga prevalent in corals of the world's hottest sea, the Persian/Arabian Gulf. *Scientific Reports*, 5(1), 8562. <https://doi.org/10.1038/srep08562>
- Hume, B., Smith, E. G., Ziegler, M., Warrington, H. J. M., Burt, J. A., LaJeunesse, T. C., ... Voolstra, C. R. (2019). SymPortal: A novel analytical framework and platform for coral algal symbiont next-generation sequencing ITS2 profiling. *Molecular Ecology Resources*, 19(4), 1063–1080. <https://doi.org/10.1111/1755-0998.13004>
- Hume, B., Voolstra, C. R., Arif, C., D'Angelo, C., Burt, J. A., Eyal, G., ... Wiedenmann, J. (2016). Ancestral genetic diversity associated with the rapid spread of stress-tolerant coral symbionts in response to Holocene climate change. *Proceedings of the National Academy of Sciences of the United States of America*, 113(16), 1601910113. <https://doi.org/10.1073/pnas.1601910113>
- Hume, B., Ziegler, M., Poulain, J., Pochon, X., Romic, S., Boissin, E., ... Voolstra, C. R. (2018). An improved primer set and amplification protocol with increased specificity and sensitivity targeting the *Symbiodinium* ITS2 region. *PeerJ*, 6, e4816. <https://doi.org/10.7717/peerj.4816>
- Jeffrey, S. W., & Humphrey, G. F. (1975). New spectrophotometric equations for determining chlorophylls a, b, c1 and c2 in higher plants, algae and natural phytoplankton. *Biochimie Und Physiologie Der Pflanzen*, 167(2), 191–194. [https://doi.org/10.1016/S0015-3796\(17\)30778-3](https://doi.org/10.1016/S0015-3796(17)30778-3)
- Jokiel, P. L. (2004). Temperature stress and coral bleaching. *Coral Health and Disease*, 401–425. [https://doi.org/10.1007/978-3-662-06414-6\\_23](https://doi.org/10.1007/978-3-662-06414-6_23)
- Jokiel, P. L., & Coles, S. L. (1977). Effects of temperature on the mortality and growth of Hawaiian reef corals. *Marine Biology*, 43(3), 201–208. <https://doi.org/10.1007/BF00402312>
- Jokiel, P. L., & Coles, S. L. (1990). Response of Hawaiian and other Indo-Pacific reef corals to elevated temperature. *Coral Reefs*, 8(4), 155–162. <https://doi.org/10.1007/BF00265006>
- Kenkel, C. D., Goodbody-Gringley, G., Caillaud, D., Davies, S. W., Bartels, E., & Matz, M. V. (2013). Evidence for a host role in thermotolerance divergence between populations of the mustard hill coral (*Porites astreoides*) from different reef environments. *Molecular Ecology*, 22(16), 4335–4348. <https://doi.org/10.1111/mec.12391>
- Kenkel, C. D., Setta, S. P., & Matz, M. V. (2015). Heritable differences in fitness-related traits among populations of the mustard hill

- coral, *Porites astreoides*. *Heredity*, 115(6), 509–516. <https://doi.org/10.1038/hdy.2015.52>
- Kozak, M., & Piepho, H.-P. (2018). What's normal anyway? Residual plots are more telling than significance tests when checking ANOVA assumptions. *Journal of Agronomy and Crop Science*, 204(1), 86–98. <https://doi.org/10.1111/jac.12220>
- Kuznetsova, A., Brockhoff, P. B., & Christensen, R. H. B. (2017). lmerTest package: Tests in linear mixed effects models. *Journal of Statistical Software*, 82(13), 2017. <https://doi.org/10.18637/jss.v082.i13>
- LaJeunesse, T. C., Parkinson, J. E., Gabrielson, P. W., Jeong, H. J., Reimer, J. D., Voolstra, C. R., & Santos, S. R. (2018). Systematic revision of Symbiodiniaceae highlights the antiquity and diversity of coral endosymbionts. *Current Biology*, 28(16), 2570–2580.e6. <https://doi.org/10.1016/j.cub.2018.07.008>
- LaJeunesse, T. C., Wham, D. C., Pettay, D. T., Parkinson, J. E., Keshavmurthy, S., & Chen, C. A. (2014). Ecologically differentiated stress-tolerant endosymbionts in the dinoflagellate genus Symbiodinium (Dinophyceae) Clade D are different species. *Phycologia*, 53(4), 305–319. <https://doi.org/10.2216/13-186.1>
- Lenth, R., Singmann, H., Love, J., Buerkner, P., & Herve, M. (2019). emmeans: Estimated marginal means, aka least-squares means. R package version 1.4.5. <https://cran.r-project.org/web/packages/emmeans/index.html>
- Lesser, M. P. (2006). Oxidative stress in marine environments: Biochemistry and physiological ecology. *Annual Review of Physiology*, 68(1), 253–278. <https://doi.org/10.1146/annurev.physiol.68.040104.110001>
- Lesser, M. P., Stochaj, W. R., Tapley, D. W., & Shick, J. M. (1990). Bleaching in coral reef anthozoans: Effects of irradiance, ultraviolet radiation, and temperature on the activities of protective enzymes against active oxygen. *Coral Reefs*, 8(4), 225–232. <https://doi.org/10.1007/BF00265015>
- Liu, G., Heron, S. F., Mark Eakin, C., Muller-Karger, F. E., Vega-Rodriguez, M., Guild, L. S., ... Lynds, S. (2014). Reef-scale thermal stress monitoring of coral ecosystems: New 5-km global products from NOAA coral reef watch. *Remote Sensing*, 6(11), 11579–11606. <https://doi.org/10.3390/rs61111579>
- Lundgren, P., Vera, J. C., Peplow, L., Manel, S., & van Oppen, M. J. H. (2013). Genotype–environment correlations in corals from the Great Barrier Reef. *BMC Genetics*, 14(1), 9. <https://doi.org/10.1186/1471-2156-14-9>
- McLachlan, R. H., Price, J. T., Solomon, S. L., & Grottoli, A. G. (2020). Thirty years of coral heat-stress experiments: A review of methods. *Coral Reefs*. <https://doi.org/10.1007/s00338-020-01931-9>
- Middlebrook, R., Hoegh-Guldberg, O., & Leggat, W. (2008). The effect of thermal history on the susceptibility of reef-building corals to thermal stress. *Journal of Experimental Biology*, 211(7), 1050–1056. <https://doi.org/10.1242/jeb.013284>
- Morikawa, M. K., & Palumbi, S. R. (2019). Using naturally occurring climate resilient corals to construct bleaching-resistant nurseries. *Proceedings of the National Academy of Sciences of the United States of America*, 116(21), 10586–10591. <https://doi.org/10.1073/pnas.1721415116>
- National Academies of Sciences Engineering & Medicine. (2019). A research review of interventions to increase the persistence and resilience of Coral Reefs. *The National Academies Press*. <https://doi.org/10.17226/25279>
- Nielsen, D. A., Petrou, K., & Gates, R. D. (2018). Coral bleaching from a single cell perspective. *The ISME Journal*, 12(6), 1558–1567. <https://doi.org/10.1038/s41396-018-0080-6>
- Oliver, T. A., & Palumbi, S. R. (2011). Do fluctuating temperature environments elevate coral thermal tolerance? *Coral Reefs*, 30(2), 429–440. <https://doi.org/10.1007/s00338-011-0721-y>
- Osman, E. O., Smith, D. J., Ziegler, M., Kürten, B., Conrad, C., El-Haddad, K. M., ... Suggett, D. J. (2018). Thermal refugia against coral bleaching throughout the northern Red Sea. *Global Change Biology*, 24(2), e474–e484. <https://doi.org/10.1111/gcb.13895>
- Palumbi, S. R., Barshis, D. J., Traylor-Knowles, N., & Bay, R. A. (2014). Mechanisms of reef coral resistance to future climate change. *Science*, 344(6186), 895–898. <https://doi.org/10.1126/science.1251336>
- Pineda, J., Starczak, V., Tarrant, A., Blythe, J., Davis, K., Farrar, T., ... da Silva, J. C. B. (2013). Two spatial scales in a bleaching event: Corals from the mildest and the most extreme thermal environments escape mortality. *Limnology and Oceanography*, 58(5), 1531–1545. <https://doi.org/10.4319/lo.2013.58.5.1531>
- R Core Team. (2019). R: A language and environment for statistical computing. Vienna, Austria: R Foundation for Statistical Computing. <https://www.r-project.org>
- Ralph, P. J., Gademann, R., & Larkum, A. W. D. (2001). Zooxanthellae expelled from bleached corals at 33°C are photosynthetically competent. *Marine Ecology Progress Series*, 220, 163–168. <https://doi.org/10.3354/meps220163>
- Roik, A., Röthig, T., Roder, C., Ziegler, M., Kremb, S. G., & Voolstra, C. R. (2016). Year-long monitoring of physico-chemical and biological variables provide a comparative baseline of coral reef functioning in the central Red Sea. *PLoS One*, 11(11), e0163939. <https://doi.org/10.1371/journal.pone.0163939>
- Rosado, P. M., Leite, D. C. A., Duarte, G. A. S., Chaloub, R. M., Jospin, G., Nunes da Rocha, U., ... Peixoto, R. S. (2019). Marine probiotics: Increasing coral resistance to bleaching through microbiome manipulation. *The ISME Journal*, 13(4), 921–936. <https://doi.org/10.1038/s41396-018-0323-6>
- Safaie, A., Silbiger, N. J., McClanahan, T. R., Pawlak, G., Barshis, D. J., Hench, J. L., ... Davis, K. A. (2018). High frequency temperature variability reduces the risk of coral bleaching. *Nature Communications*, 9(1). <https://doi.org/10.1038/s41467-018-04074-2>
- Schloss, P. D., Westcott, S. L., Ryabin, T., Hall, J. R., Hartmann, M., Hollister, E. B., ... Weber, C. F. (2009). Introducing mothur: Open-source, platform-independent, community-supported software for describing and comparing microbial communities. *Applied and Environmental Microbiology*, 75(23), 7537–7541. <https://doi.org/10.1128/AEM.01541-09>
- Stimson, J., & Kinzie, R. A. (1991). The temporal pattern and rate of release of zooxanthellae from the reef coral *Pocillopora damicornis* (Linnaeus) under nitrogen-enrichment and control conditions. *Journal of Experimental Marine Biology and Ecology*, 153(1), 63–74. [https://doi.org/10.1016/S0022-0981\(05\)80006-1](https://doi.org/10.1016/S0022-0981(05)80006-1)
- van Woesik, R., Houk, P., Isechal, A. L., Idechong, J. W., Victor, S., & Golbuu, Y. (2012). Climate-change refugia in the sheltered bays of Palau: Analogs of future reefs. *Ecology and Evolution*, 2(10), 2474–2484. <https://doi.org/10.1002/ece3.363>
- van Woesik, R., Sakai, K., Ganase, A., & Loya, Y. (2011). Revisiting the winners and the losers a decade after coral bleaching. *Marine Ecology Progress Series*, 434, 67–76. Retrieved from <https://www.int-res.com/abstracts/meps/v434/p67-76/>
- Warner, M. E., Fitt, W. K., & Schmidt, G. W. (1996). The effects of elevated temperature on the photosynthetic efficiency of zooxanthellae in hospite from four different species of reef coral: A novel approach. *Plant, Cell & Environment*, 19(3), 291–299. <https://doi.org/10.1111/j.1365-3040.1996.tb00251.x>
- Warner, M. E., Lesser, M. P., & Ralph, P. J. (2010). Chlorophyll fluorescence in reef building corals BT. In D. J. Suggett, O. Prášil, & M. A. Borowitzka (Eds.), *Chlorophyll a fluorescence in aquatic sciences: Methods and applications* (pp. 209–222). Netherlands: Springer. [https://doi.org/10.1007/978-90-481-9268-7\\_10](https://doi.org/10.1007/978-90-481-9268-7_10)
- Winters, G., Holzman, R., Blekhan, A., Beer, S., & Loya, Y. (2009). Photographic assessment of coral chlorophyll contents: Implications for ecophysiological studies and coral monitoring. *Journal of Experimental Marine Biology and Ecology*, 380(1), 25–35. <https://doi.org/10.1016/j.jembe.2009.09.004>
- Ziegler, M., Seneca, F. O., Yum, L. K., Palumbi, S. R., & Voolstra, C. R. (2017). Bacterial community dynamics are linked to patterns of

coral heat tolerance. *Nature Communications*, 8, 1–8. <https://doi.org/10.1038/ncomms14213>

## SUPPORTING INFORMATION

Additional supporting information may be found online in the Supporting Information section.

**How to cite this article:** Voolstra CR, Buitrago-López C, Perna G, et al. Standardized short-term acute heat stress assays resolve historical differences in coral thermotolerance across microhabitat reef sites. *Glob Change Biol*. 2020;26: 4328–4343. <https://doi.org/10.1111/gcb.15148>